JOURNAL OF SOLID STATE CHEMISTRY 93, 461–468 (1991)

Structural Change and Magnetic Properties of $Y_2BaNi_{1-x}Zn_xO_5$ Oxides

R. SAEZ-PUCHE,* J. M. CORONADO, AND C. L. OTERO-DÍAZ

Departamento Química Inorgánica, Facultad de Ciencias Químicas, Universidad Complutense, 28040 Madrid, Spain

AND J. M. MARTÍN LLORENTE

Departamento Química Inorgánica, Facultad de Ciencias Químicas, Universidad de Salamanca, Salamanca (Spain)

Received January 9, 1991

The magnetic susceptibility of Y_2BaNiO_5 has been measured in the range 4.2–800 K. The broad maximum in the χ vs T plot centered at 420 K is indicative of the existence of low-dimensional antiferromagnetic ordering along the chains of vertex sharing (NiO_6) octahedra in the a-axis of the structure. The data have been fitted by using the 1D Heisenberg model and the value of the exchange constant J is -322 K. Doped $Y_2BaNi_{1-x}Zn_xO_5$ oxides have also been prepared and the Y_2BaNiO_5 structure changes, giving rise to the Sm_2BaCuO_5 structure type, characterized by the existence of isolated pyramids (CuO_5), for x values as small as 0.13. Electron microscopy and diffraction studies reveal the existence of a well-ordered microstructure with the Zn and Ni atoms randomly distributed.

Introduction

The oxide Y_2BaNiO_5 recently characterized by single crystal X-ray diffraction (*1*, *2*) adopts the Nd_2BaNiO_5 structure type (*3*), space group *Immm;* it is built up by isolated chains of corner-sharing flattened octahedra, running parallel to the c-axis. Further studies confirmed the same structure for the different R_2BaNiO_5 oxides with R from Nd to Tm (*3*, *4*). In the case of the smallest trivalent rare earth cations, Yb^{3+} and Lu^{3+}, the corresponding oxides are isostructural (*4*, *5*), showing the Sm_2BaCuO_5 structure type (*5*, *6*), space group *Pbnm*, where the lanthanoid ions are 7-coordinated by oxygen atoms in a monocapped trigonal prism, while the Cu^{2+} ions are 5-coordinated, forming isolated distorted square pyramids (CuO_5), and the Ba ions are surrounded by 11 oxygen ions in a tricapped distorted square prism. The lanthanoid polyhedra (YO_7) form units of (Y_2O_{11}) chains, which are connected by the Cu polyhedra using an edge and a triangular face for the different chains.

Evidence of low-dimensional antiferromagnetic ordering has been reported for Y_2BaNiO_5 (*1*, *7*). This behavior was explained by the existence of strong superexchange Ni–O–Ni at 180° interactions along the chains of flattened (NiO_6) octahedra. In

* To whom correspondence should be addressed.

0022-4596/91 $3.00

order to break down the observed one-dimensional antiferromagnetic ordering for the Y_2BaNiO_5, substituted $Y_2BaNi_{1-x}Zn_xO_5$ oxides were prepared.

We report in this work results on the $Y_2BaNi_{1-x}Zn_xO_5$ system studied by X-ray powder diffraction, electron microscopy, and magnetic susceptibility measurements.

Experimental

Powder samples of Y_2BaNiO_5 and doped phases $Y_2BaNi_{1-x}Zn_xO_5$ were prepared from stoichiometric mixtures of high purity Y_2O_3 (99.99%), NiO (99.99%), and $BaCO_3$ (A.R.) and ZnO (A.R.). The ground powders were heated in air at 1200°C for 48 hr with several interruptions for regrinding.

X-ray data were obtained in a Siemens K810 powder diffractometer using Cu$K\alpha$ radiation and a D-501 goniometer provided with a secondary graphite monochromator. The data were analyzed by using the Rietveld refinement method (*8*).

Specimens (dispersed on holey carbon films on Cu grids) were studied by electron microscopy/diffraction in a JEOL 2000-FX instrument, fitted with an AN 10000 LYNK and a double tilt range ±45° to explore the reciprocal space, and in a JEOL 4000 EX for high-resolution imaging.

Magnetic susceptibility measurements were performed in the temperature range 4–800 K by the Faraday method. The maximum field was 14 kG and HdH/dz = 24 $kG^2\,cm^{-1}$. The data were corrected for ionic diamagnetism using the values of -16×10^{-6} emu $mole^{-1}$ for O^{2-}, -31×10^{-6} for Ba^{2+}, and -12×10^{-6} for Ni^{2+} and Zn^{2+} (*9*).

Results and Discussion

Unit cell parameters of the Y_2BaNiO_5 sample using the Rietveld refinement method are a = 3.7398(1) Å, b = 5.7594(2) Å, c = 11.3294(4) Å, and V = 245.33(4) Å^3, in good agreement with the previous single-crystal data reported earlier (*1*).

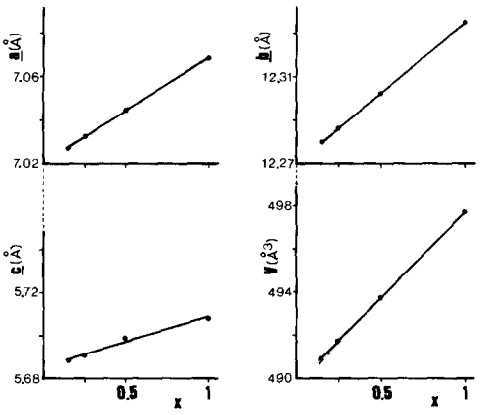

FIG. 1. Unit cell parameters versus composition for the different $Y_2BaNi_{1-x}Zn_xO_5$ samples.

In order to study the influence of the substitution of Ni by the diamagnetic Zn on the structural and magnetic properties, different substituted samples with nominal composition $Y_2BaNi_{1-x}Zn_xO_5$, x = 0.10, 0.15, 0.25, 0.50, and 1, have been synthetized. X-ray diffraction data revealed that for x values as small as 0.15 a structural change takes place and the obtained phase shows the Sm_2BaCuO_5 structure type (*5*, *6*).

Figure 1 shows the expected tendency for the unit cell axes and volume to increase with increasing x in $Y_2BaNi_{1-x}Zn_xO_5$ due to the ionic sizes (Ni^{2+} = 0.61 Å and Zn^{2+} = 0.68 Å both in 5-coordination (*11*)). The linear relationship between both magnitudes suggests the existence of a homogeneous solid solution in the composition range $0.15 \leq x \leq 1$.

The X-ray diffraction pattern of the sample of nominal composition $Y_2BaNi_{0.9}Zn_{0.1}O_5$, Fig. 2, shows the presence of a majority phase, $Y_2BaNi_{1-x}Zn_xO_5$, with the Y_2BaZnO_5 structure type and some of the higher intensity reflections of the Y_2BaNiO_5 oxide. The lattice parameters of the former have been calculated by fitting the pattern

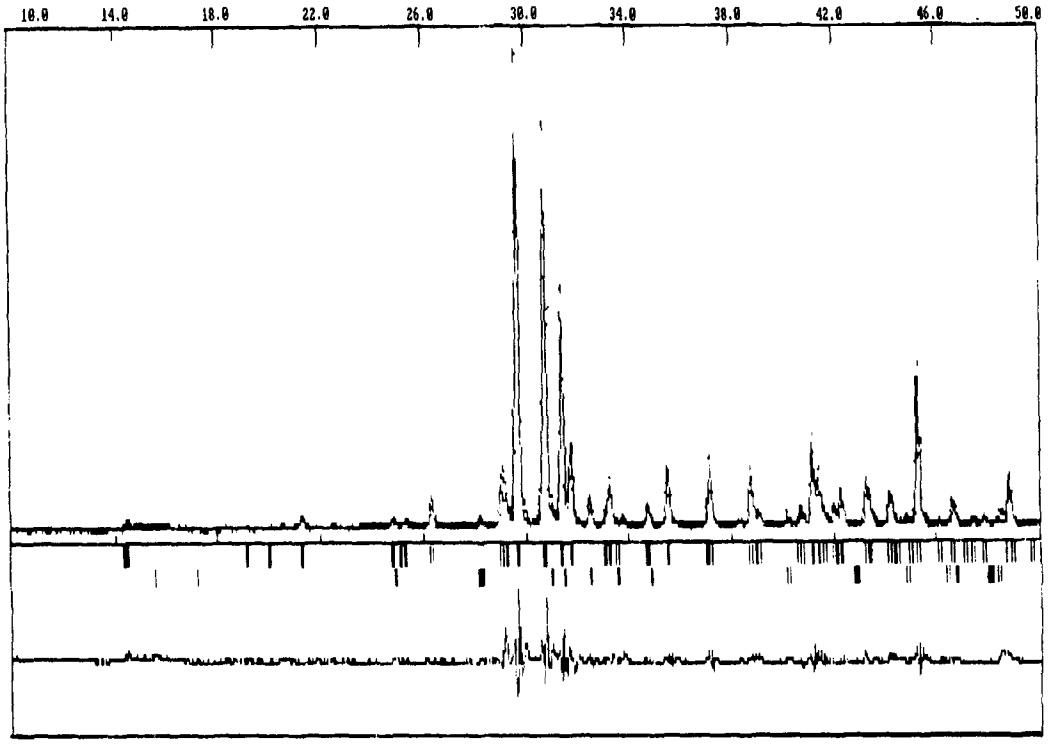

FIG. 2. X-ray diffraction pattern for the sample of nominal composition $Y_2BaNi_{0.9}Zn_{0.1}O_5$. Points represent the experimental data and the solid line is the calculated profile. A difference curve is plotted at the bottom of the pattern. The first and the second series of Bragg reflection markers correspond to the crystal structures of $Y_2BaNi_{0.87}Zn_{0.13}O_5$ and Y_2BaNiO_5, respectively.

with the Rietveld method, Fig. 2, and the obtained lattice parameters are $a = 7.0262(4)$ Å, $b = 12.2791(6)$ Å, and $c = 5.6884(3)$ Å. The extrapolation of these lattice constants shown in the straight lines in Fig. 1 yields an average value of x for the unknown $Y_2BaNi_{1-x}Zn_xO_5$ oxide of 0.13 which permits us to suggest that the lower solid solution limit for these mixed oxides corresponds to that for the sample with nominal composition $Y_2BaNi_{0.87}Zn_{0.13}O_5$.

In order to study the microstructure of this solid solution, samples with different proportions of Zn have been analyzed by conventional transmission electron microscopy, which is a more sensitive technique to detect ordering–disordering structural details. However, in all the samples, including the $Y_2BaNi_{0.5}Zn_{0.5}O_5$, neither streaks nor superlattice reflections can be seen in the selected area diffraction patterns and corresponding images.

Figure 3 shows two electron diffraction patterns from the same crystal of the sample with nominal composition $Y_2BaNi_{0.5}Zn_{0.5}O_5$. Zone axes are indicated. The absence of extra reflections or weak scattering indicates the nonexistence of long-/short-range order between both types of ions. Figure 4b shows a high-resolution image at the unit cell level from a crystal of the sample with nominal composition $Y_2BaNi_{0.75}Zn_{0.25}O_5$, taken with the incident beam parallel to the short axis of the structure; see

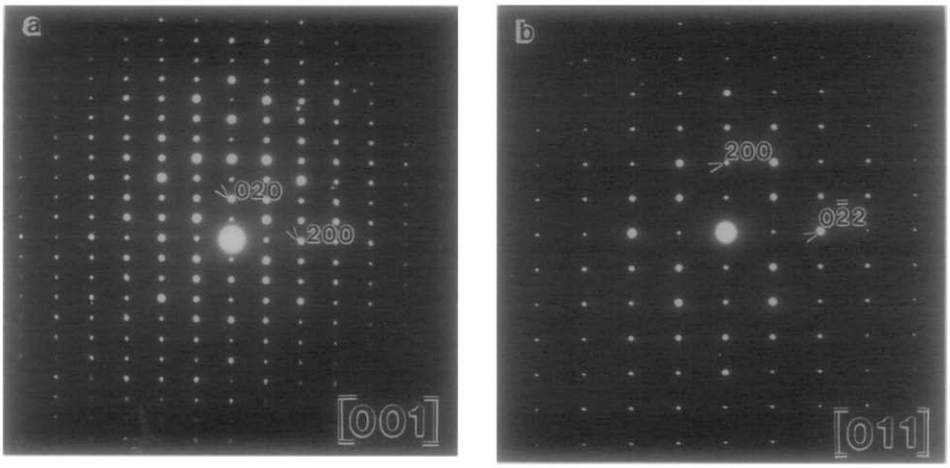

FIG. 3. Electron diffraction patterns from the same crystal of the sample with nominal composition $Y_2BaNi_{0.5}Zn_{0.5}O_5$. Zone axes are indicated.

diffraction pattern in Fig. 4a. The contrast is rather uniform, without any structural defects, changing only with the crystal thickness. These preliminary results suggest that both ions Zn^{2+} and Ni^{2+} are distributed in a random way in the solid solution with $0.13 \leq x \leq 1$.

On the other hand, Fig. 5 corresponds to a high-resolution image (a) and diffraction pattern (b) from a crystal of the pure

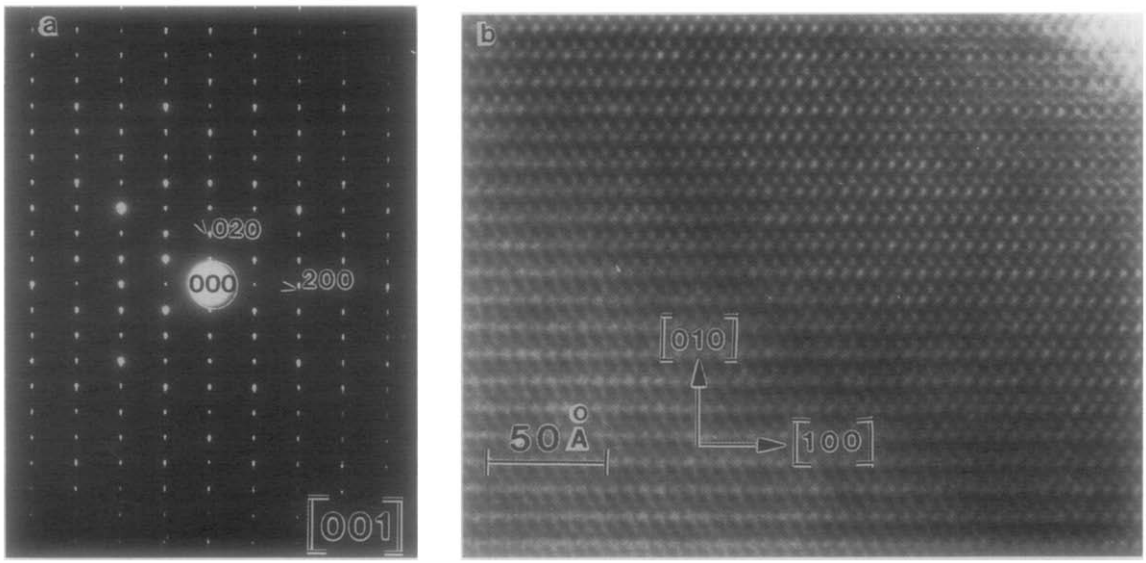

FIG. 4. (a) Electron diffraction pattern from a crystal of the sample $Y_2BaNi_{0.75}Zn_{0.25}O_5$ along the [001] orientation. (b) High-resolution lattice image of the same crystal along the c-axis (orientation is given in (a)).

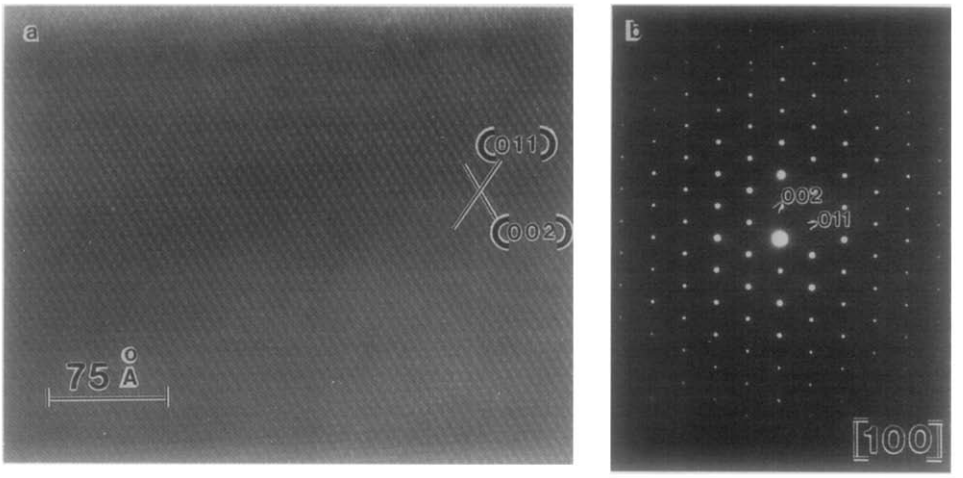

FIG. 5. Lattice image (a) and corresponding diffraction pattern (b) from a crystal flake of the sample Y_2BaNiO_5 showing the uniform contrast typical of a well-ordered structure. Zone axis has been indicated.

Y_2BaNiO_5 phase; the zone axis is [100]. The contrast observed in the micrograph is typical of a well-ordered structure. The traces of (002) and (011) planes with 5.7 and 5.1 Å, respectively, have been marked on it.

The XEDS analysis confirms semiquantitatively the nominal composition for the studied $Y_2BaNi_{1-x}Zn_xO_5$ samples.

Figure 6 shows the variation of the molar magnetic susceptibility versus temperature for Y_2BaNiO_5. The broad maximum centered at 420 K confirms the expected one-dimensional behavior as a consequence of the linear isolated chains of corner-sharing (NiO_6) octahedra mentioned earlier (*1*). The experimental data have been corrected taking into account a small paramagnetic contribution that was observed below 40 K and using a Curie constant value of 0.059 emu · mole^{-1} · K.

Interactions between magnetic ions can be described in terms of the spin Hamiltonian by

$$\mathcal{H} = -2J \sum_{i=1}^{N} [S_i^z S_{i+1}^z + \gamma(S_i^x S_{i+1}^x + S_i^y S_{i+1}^y)],$$

where S_i^z, S_i^y, and S_i^x are the components of the spin operator and J is the exchange constant. The Heisenberg model is obtained when $\gamma = 1$, which corresponds to an isotropic exchange interaction (*10*). Although there is no exact solution for the susceptibility for such a system, we have used the expression based on the numerical results given by Weng (*11*) for linear chains with $S = 1$, which takes the form

$$\frac{\chi|J|}{Ng^2\beta^2} = \frac{2x + 0.0302x^2 + 0.8997x^3}{3 + 5.4452x + 2.7477x^2 + 6.9038x^3},$$

where $x = |J|/K_BT$. Assuming that J and g can vary, the best agreement between theoretical and experimental data is obtained for $g = 2.60$ and $J/K_B = -322$ K. The solid line in Fig. 6 is the fitted curve. The agreement criterion using R for the theoretical curve has been defined as the sum of the squares of the relative deviation, and the R value obtained is 8.44×10^{-5}. The validity of the Heisenberg model appears to be justified because both theoretical and experimental susceptibility data take a finite value when

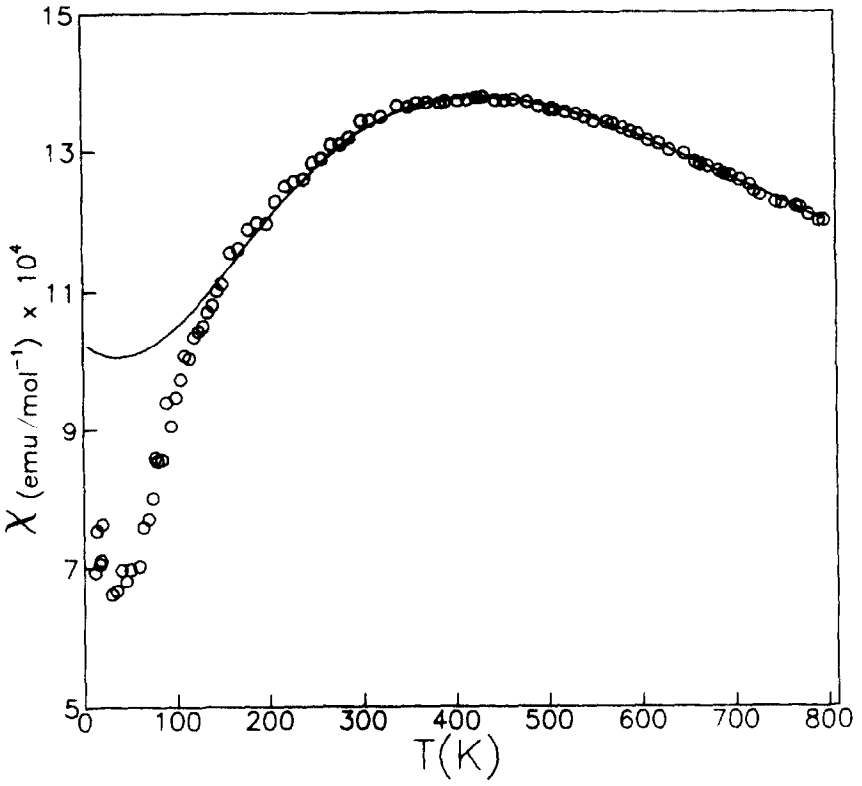

FIG. 6. Temperature dependence of the molar magnetic susceptibility for Y_2BaNiO_5. The solid line represents the calculated magnetic susceptibility by using Weng's equation and open circles represent the experimental data.

the temperature approaches zero. However, the fully anisotropic Ising model (*12*), derived from the same Hamiltonian given above, taking $\gamma = 0$, does not describe our system because in the low-temperature range the susceptibility approaches zero. Although the obtained g value is much larger than expected for Ni^{2+} in an octahedral environment (*13*) this could be due to the strong distortion found in the (NiO_6) octahedra that is likely to be important in our case but can be neglected as a first approximation.

Neutron diffraction studies (*14*) down to 1.5 K do not reveal the existence of long-range antiferromagnetic ordering which confirms our statement about the one-dimensional magnetic behavior of the Y_2BaNiO_5.

Figure 7 shows the temperature dependence of the molar magnetic susceptibility of the sample with nominal composition $Y_2BaNi_{0.75}Zn_{0.25}O_5$. It can be observed that the susceptibility follows a Curie–Weiss law between 300 and 50 K and the calculated magnetic moment, 3.0 BM, agrees with that expected for isolated Ni^{2+} ions. Below 50 K the susceptibility increases and at 10 K it remains almost constant, which is indicative that at these low temperatures antiferromagnetic interactions between Ni^{2+} ions are operative. This effect is even more clearly visualized when $\chi \times T$ vs T is plotted, Fig. 7

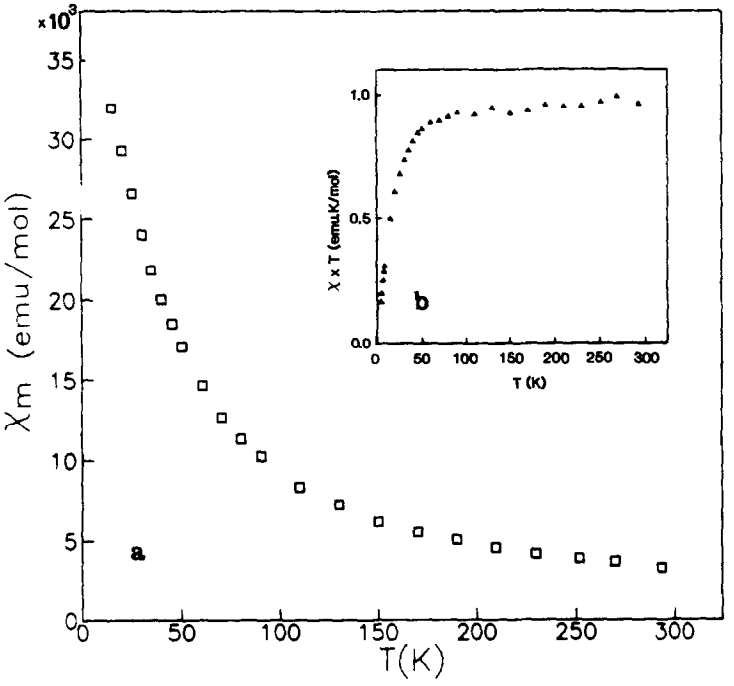

FIG. 7. Temperature dependence of the molar magnetic susceptibility for $Y_2BaNi_{0.75}Zn_{0.25}O_5$. The $\chi \times T$ vs T plot is shown in the inset.

inset; a marked decrease in the $\chi \times T$ value with decreasing temperature can be observed, reaching a rather small value of only 0.15 emu · K · mole^{-1} at 4.2 K. Similar results have been reported for the isostructural Y_2BaCuO_5 (*15, 16*), although the Néel temperature, 28 K, is higher than the value obtained for these doped phases. The low temperature at which the three-dimensional magnetic interactions are acting is not surprising since the possible superexchange pathways will be of the form Ni–O–Y (Ba)–O–Ni with angles very different from 180°, giving rise to weak interactions. In addition, the random substitution of Ni by Zn, as, for example, in the sample $Y_2BaNi_{0.75}Zn_{0.25}O_5$, Fig. 7, obviously diminishes these interactions, lowering the Néel temperature.

Neutron diffraction studies are now in progress in order to determine the magnetic structure and the Néel temperature of these doped oxides.

Acknowledgments

We thank the Centro de Microscopía Electrónica (U.C.M.) for the use of its facilities and Dr. J. C. Grenier (Bordeaux, France) for the high-temperature measurements. This research was supported by the CYCI project MAT 89-0768.

References

1. J. AMADOR, E. GUTIÉRREZ-PUEBLA, M. A. MONGE, I. RASINES, C. RUIZ-VALERO, F. FERNÁNDEX, R. SÁEZ-PUCHE, AND J. A. CAMPÁ, *Phys. Rev. B* **42**(13), 4337 (1990).
2. D. J. BUTTREY, J. D. SULLIVAN, AND A. L. RHEINGOLD, *J. Solid State Chem.* **88**, 291 (1990).
3. S. SCHIFFLER AND H. MÜLLER-BUSCHBAUM, *Z. Anorg. Allg. Chem.* **532**, 10 (1986).

4. S. SHIFFLER AND H. MÜLLER-BUSCHBAUM, *Monatsh. Chem.* **118,** 741 (1986).
5. H. MÜLLER-BUSCHBAUM AND I. RÜTER, *Z. Anorg. Allg. Chem.* **540,** 243 (1986).
6. C. MICHEL AND B. RAVEAU, *J. Solid State Chem.* **43,** 73 (1982).
7. R. SÁEZ-PUCHE, J. M., CORONADO-CARNEIRO, C. L., OTERO-DIÁZ, AND J. M. MARTIN-LLORENTE, *Eur. J. Solid State Inorg. Chem.*, in press.
8. J. RODRÍGUEZ-CARVAJAL, "FULLPROF: A Program for Rietveld Refinement and Pattern Matching Analysis," Abstract of the Satellite Meeting of the 15th Congress of the International Union of Crystallography, p. d-127, Toulouse, France (1990).
9. L. N. MULAY AND E. A. BOUDREAUX (Eds.), "Theory of Molecular Paramagnetism," p. 494, Wiley, New York (1976).
10. L. J. DE JONGH AND A. R. MIEDEMA, *Adv. Phys.* **23,** 1 (1974).
11. C. Y. WENG, Ph.D. thesis, Carnegie Institute of Technology (1968).
12. E. ISING, *Z. Phys.* **31,** 253 (1925).
13. R. L. CARLING, "Magnetochemistry," Springer-Verlag, Berlin/Heidelberg (1986).
14. J. L. MARTÍNEZ, personal communication.
15. T. CHATTOPADHYAY, P. J. BROWN, W. KÖBLER, AND M. WILHELM, *Europhys. Lett.* **8,** 685 (1989).
16. A. SALINAS-SÁNCHEZ, R. SÁEZ-PUCHE, AND M. A. ALARIO-FRANCO, *J. Solid State Chem.*, in press.